Communications and Network, 2023, 15, 83-97
https://www.scirp.org/journal/cn
ISSN Online: 1947-3826
ISSN Print: 1949-2421

Impact of Heat Treatments and Hole Density (p) on the Structural, Electrical, and Superconducting Properties of $LnSrBaCu_3O_{6+z}$ (Ln = Eu, Sm, Nd) Compounds

Mohammed Bellioua[1], Mohamed Id El Amel[1], Fatima Bouzit[1], Mohamed Errai[1,2], Driss Soubane[3,4], Aderrahim Ait Khlifa[1], Mohammed Khenfouch[1], Issam Mouhti[1], Ahmed Tirbiyine[1], Essediq Youssef El Yakoubi[5], Abdelhakim Nafidi[5]

[1]Laboratory of Materials, Electrical Systems, Energy and Environment, Department of Applied Physics, Faculty of Applied Sciences, Ibnou Zohr University, Agadir, Morocco
[2]LAMISNE Laboratory, Polydisciplinary Faculty of Taroudant, Ibn Zohr University, Agadir, Morocco
[3]Department of Physics, Polydisciplanry Faculty Safi, Cadi Ayyad University, Marrakech, Morocco
[4]ALLS Laboratory at INRS-EMT, Varennes, Canada
[5]Laboratory of Condensed Matter Physics and Nanomaterials for Renewable Energy, Faculty of Sciences, Agadir, Morocco
Email: mbellioua@yahoo.fr

How to cite this paper: Bellioua, M., El Amel, M.I., Bouzit, F., Errai, M., Soubane, D., Khlifa, A.A., Khenfouch, M., Mouhti, I., Tirbiyine, A., El Yakoubi, E.Y. and Nafidi, A. (2023) Impact of Heat Treatments and Hole Density (p) on the Structural, Electrical, and Superconducting Properties of $LnSrBaCu_3O_{6+z}$ (Ln = Eu, Sm, Nd) Compounds. *Communications and Network*, **15**, 83-97.
https://doi.org/10.4236/cn.2023.154006

Received: August 7, 2023
Accepted: September 24, 2023
Published: September 27, 2023

Abstract

In this study, we thoroughly examined the impact of heat treatments and hole count (p) on the properties of $LnSrBaCu_3O_{6+z}$ (Ln = Eu, Sm, Nd) compounds. We focused on preparation, X-ray diffraction with Rietveld refinement, AC susceptibility, DC resistivity measurements, and heat treatment effects. Two heat treatment types were applied: oxygen annealing [O] and argon annealing followed by oxygen annealing [AO]. As the rare earth Ln's ionic radius increased, certain parameters notably changed. Specifically, c parameter, surface area S, and volume V increased, while critical temperature Tc and holes (p) in the CuO_2 plane decreased. The evolution of these parameters with rare earth Ln's ionic radius in [AO] heat treatment is linear. Regardless of the treatment, the structure is orthorhombic for Ln = Eu, tetragonal for Ln = Nd, orthorhombic for Ln = Sm [AO], and pseudo-tetragonal for Sm [O]. The highest critical temperature is reached with Ln = Eu (Tc [AO] = 87.1 K). Notably, for each sample, Tc [AO] surpasses Tc [O]. Observed data stems from factors including rare earth ionic size, improved cationic and oxygen chain order, holes count p in $Cu(2)O_2$ planes, and in-phase purity of [AO] samples. Our research strives to clearly demonstrate that the density of holes (p) within the copper plane stands as a determinant impacting the structural, electrical, and superconducting properties of these samples. Meanwhile, the other aforementioned parameters contribute to shaping this density (p).

Keywords

High-Tc Superconductors, Heat Treatments, Hole Density (p), Tc, Parameter c, Surface ab, Electrical Resistance, X-Ray Diffraction

1. Introduction

Since the late 1980s, with the discovery of high-temperature superconductors [1], considerable attention has focused on substituting atoms within them. The superconductive prototype $YBa_2Cu_3O_{6+z}$, reaching a critical temperature Tc = 93 K [2], has emerged from these substitutions. These substitutions influence the prototype's atoms, affecting the number of holes (p) in the $Cu(2)O_2$ superconductive plane. Experimental evidence supports that these holes have a pivotal role in achieving a high critical temperature, thus optimizing the $Cu(2)O_2$ plane conditions in these cuprates [3] [4] [5] [6].

The critical temperature of $LnBaSrCu_3O_{6+z}$ samples involving rare earths, as reported by multiple authors [7] [8] [9], is solely dependent on the ion size of the rare earth element. We studied the structural and superconductive properties of $SmSrBaCu_3O_{6+z}$ [10]. Annealing this compound in oxygen at 450˚C revealed a tetragonal structure and Tc of 79 K. Subjecting the same sample to argon heating and subsequent oxygen annealing unveiled an orthorhombic structure with a Tc increase of 6 K. We also establish that the structure is orthorhombic for $EuSrBaCu_3O_{6+z}$ and tetragonal for $NdSrBaCu_3O_{6+z}$, irrespective of thermal treatment. Heat treatment under argon heightens the critical temperature (Tc [AO] > Tc [O]), underscoring Tc's dependence on thermal processing.

Our study assesses how the quantity of holes (p) in $Cu(2)O_2$ planes affects structural, electrical, and superconductive properties of our samples.

2. Experimental Techniques

The respective oxides and carbonates were solid-state sintered to prepare the polycrystalline samples. The chemicals were of 99.999% purity, with the exception of $BaCO_3$, which had a purity of 99.99%. Were meticulously blended in necessary proportions and subjected to calcination at 950˚C in the air for a duration of 12 - 18 hours. The product obtained was ground, pelletized, and subjected to air heating at 980˚C for 16 - 24 hours. The pellets were annealed in oxygen at 450˚C for a period of 60 - 72 h and furnace cooled. This was denoted as sample [O] for each Ln. XRD data of the sample were collected with Philips diffractometer fitted with a secondary beam graphite monochromator and using CuKα (40 kV/20 mA) radiation. The angle 2θ, was varied from 20˚ to 120˚ in steps of 0.025˚ and the courting time per step was 10 sec. The XRD specters were refined with Rietveld refinement [11]. Superconducting transitions were checked by measuring both the real, $\chi'$and the imaginary χ''parts of the AC susceptibility as a function of temperature in a field of 0.11 Oe and at a frequency of 1500 Hz.

For each Ln, the same sample [O] was then heated in argon at 850˚C for about 12 h, cooled to 20˚C, and oxygen was allowed to flow instead of argon and the sample was annealed at 450˚C for about 72 h. This sample is represented as [AO]. XRD and AC susceptibility measurements were performed on a part of this sample. The resistivity ρ(T) was measured by the Van Der Pauw method [12]. Using a cryostat with closed helium circuit supplied of a cryogenic pump, a regulator of temperature (1 μA - 10 mA) and 1 μV resolution digital voltmeter that was fully computer controlled. The same sample [O] was then heated in argon at 850˚C for about 12 h, cooled to 20˚C, oxygen was allowed to flow instead of argon, and the sample was annealed at 450˚C for about 72 h. This sample is denoted as [AO]. XRD, susceptibility, and resistivity measurements were conducted on a portion of this sample.

3. Results and Discussion

The magnetic susceptibility AC allows studying the dynamics of the system, which gives information about the relaxation processes in the superconductor. The real part χ' gives an expression for flux that penetrates the sample. In the case of complete field expulsion (Meissner effect), $\chi' = -1$ and for total flow penetration, $\chi' = 0$. In the superconducting state, the imaginary part $\chi'' = 0$ and in the mixed state $\chi'' < 1$ and reflects losses AC.

In **Figure 1(a)**, we present the real part of the AC susceptibility (χ') for the samples [AO]. The data is plotted as a function of temperature, with the measurements taken under the influence of two externally applied DC fields. In the case of Ln = Eu [AO], we obtained the maximum critical temperature Tc = 87.1 K in $LnSrBaCu_3O_{6+z}$. It is above the maximum critical temperature 86 K obtained by [7] and below 89 K measured by B. Hellebrand *et al.* [13] in $GdBaSrCu_3O_{6+z}$. In the Nd case, the application of the [AO] treatment resulted in a significant enhancement of Tc by 10 K, elevating it from 68 K to 78 K. Remarkably, this increase in Tc did not alter the crystal symmetry, which remained tetragonal throughout the process, and there was no variation in the oxygen content either. Moreover, our computation indicated a rise in the hole density (p) following the [AO] treatment.

The peak moves to lower temperatures as the Hdc field increase from 0 to 126.5 Oe, for each Ln **Figure 1(b)**. The data for the crystalline and superconducting properties of $LnSrBaCu_3O_{6+z}$, varying with the heat treatment, can be found in **Table 1**.

The highest temperature is achieved in the scenario where the $EuSrBaCu_3O_{6+z}$ [AO] compound adopts an orthorhombic structure, whereas the lowest temperature is observed when the $NdSrBaCu_3O_{6+z}$ [O] compound takes on a tetragonal structure.

The relationship between lattice parameters “a” and “b” and the critical temperature “Tc” exhibits a linear evolution during heat treatment [AO]. The slope of the b [AO] (Tc) curve is small (Equation (1)), which shows that b is almost constant.

Table 1. The variation of crystalline and superconducting parameters in $LnSrBaCu_3O_{6+z}$ as a function of the heat treatment.

Ln	H.treat	a(Å)	b(Å)	c(Å)	$\varepsilon(10^{-3})$	a/b	Tc(K)
Eu	[O]	3.8233	3.8455	11.585	2.89485	0.99423	81.1
	[AO]	3.8021	3.8695	11.584	8.78565	0.98258	87.1
Sm	[O]	3.8464	3.8493	11.612	0.37683	0.9992	79
	[AO]	3.8232	3.8672	11.600	5.72142	0.98862	84.6
Nd	[O]	3.8672	3.8672	11.649	0	1	68
	[AO]	3.8670	3.8672	11.655	0.02586	0.99995	78

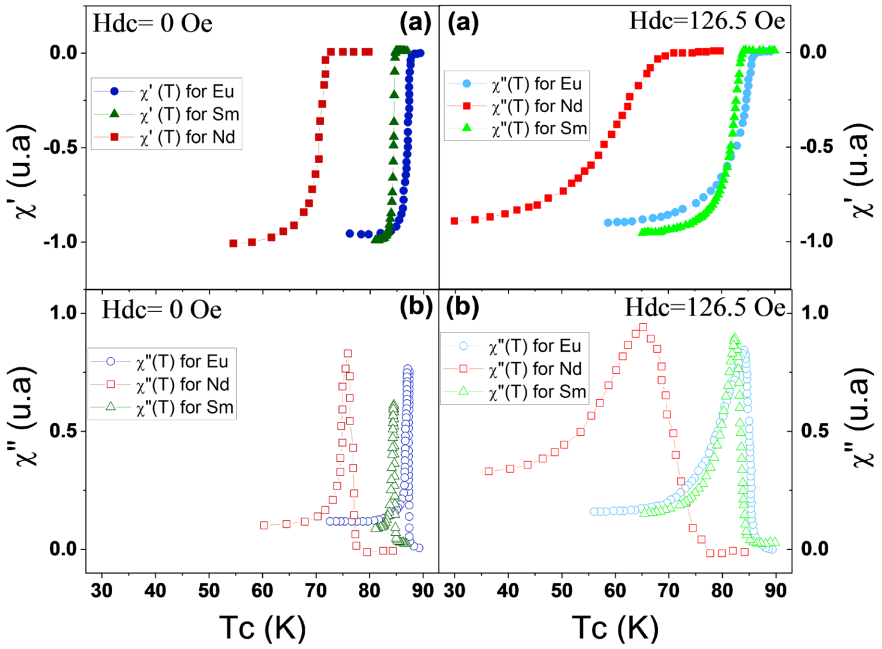

Figure 1. The temperature and heat treatment effects on the χ'(a) and χ''(b) of $LnSrBaCu_3O_{6+z}$ [AO] (Ln = Eu, Sm, Nd) were studied under two different Hdc fields (Hdc = 0 Oe and 126.5 Oe).

The other parameters b [O], a [O] and a [AO] decrease when the critical temperature Tc increases **Figure 2(a)**.

$$b[AO] = 2.012\times10^{-4}\,Tc[AO] + 3.85122 : (Å) \quad (1)$$

The fit of the points of curve a/b [AO] (Tc) gives the following equations:

$$a/b[AO] = -0.00187\,Tc[AO] + 12.53186 \quad (2)$$

The structure of the $LnSrBaCu_3O_{6+z}$ (Ln = Nd [O], Nd [AO] or Sm [O]) compounds is tetragonal (a/b ≈ 1), In contrast to the orthorhombic crystal structure (a/b ≠ 1) observed in $LnSrBaCu_3O_{6+z}$ compounds (where Ln represents Eu [O], Eu [AO], or Sm [AO]), **Figure 2(b)**. Heat treatment [AO] changed the tetragonal structure of the sample $SmSrBaCu_3O_{6+z}$ [O] to an orthorhombic structure of the sample $SmSrBaCu_3O_{6+z}$ [AO]. Therefore, the structural properties also depend on heat treatment.

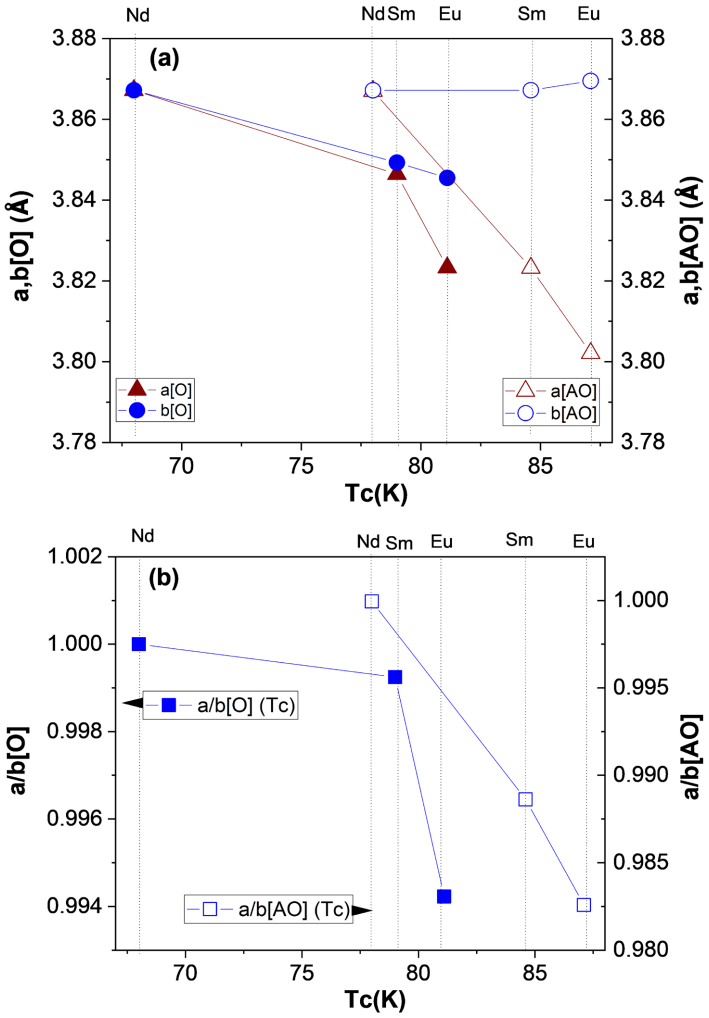

Figure 2. Lattice parameters a and b (a), and the ratio of a/b (b) as a function of the critical temperature and heat treatment of $LnSrBaCu_3O_{6+z}$.

The superconductors' oxides exhibit a remarkable feature—a high critical temperature Tc, which is profoundly influenced by the concentration of holes present on the two-dimensional layers $Cu(2)O_2$. The universal relation between standardized Tc ($\pi c = Tc/Tc_{max}$) and the concentration p of the holes in the $Cu(2)O_2$ plane of superconductors oxides (La214, Y123, Bi2212, Bi2223, Tl2201 and Tl1212) shows that Tc independent of the considered sample [3].

The hole density (p) in the $Cu(2)O_2$ planes as a function of Tc, can be inferred using the following relationship [14] [15]:

$$p = 0.16 - \left(\left(1 - \frac{Tc}{Tc_{max}}\right) \Big/ 82.6\right)^{1/2} \tag{3}$$

The Tc_{max} parameter represents the maximum critical temperature equal to 93 K in the case of cuprates.

Note here that this relation is deducted from the universal relation Tc/Tc_{max} (p) given by [4]. We used this universal relationship to infer the number of holes in

our Y1-xSmxBaSrCu$_3$O$_{6+z}$ compounds [16].

Figure 3 shows the critical temperature Tc as a function of p. The increase of p from 0.10295 for Nd [O] or Tc = 68 K to 0.13229 for Eu [AO] or Tc = 87.1 K indicates that the critical temperature Tc increases with the hole density (p) in the Cu(2)O$_2$ planes. The look of this figure is characterized by a sharp increase of Tc, with hole content in the range $0.06 < p < 0.16$ [17] [18] [19].

The impact of holes density (p) on the superconducting properties in our samples is clearly remarkably in this figure. The addition of oxygen or the substitution of isovalentcations generally leads to changes in the superconducting Cu(2)O$_2$ planes' charge density, which, in turn, affects the evolution of Tc. The maximum Tc occurs at the optimum p value of ~0.15 - 0.16 for several compounds.

A correlation has been established between the number of holes (p) and the critical temperature (Tc) as function of the lattice parameter (c) and heat treatment in LnSrBaCu$_3$O$_{6+z}$ (Ln = Eu, Nd, Sm) as depicted in Figure 4. An almost linear curve is obtained when plotting the p [AO] values as a function of the c [AO]-axis values. The fit of the points gives the following equations:

$$p[\mathrm{AO}] = -0.22448\,c[\mathrm{AO}] + 22.88536 \tag{4}$$

These authors are shown in the phase diagram that temperature as a function of hole doping, (p) and as a function of oxygen content, (y) superconducting YBa$_2$Cu$_3$O$_y$ prototype are correlated. The negative slope of the concentration (p) of holes in the Cu(2)O$_2$ planes as a function of the lattice parameter (c) during heat treatment under argon (Equation (4)) compared by the slope of oxygen content, (y) as a function of this parameter in the case of YBa$_2$Cu$_3$O$_y$ obtained by several authors [20] [21] [22]. The augmented oxygen content in the Cu(1)O basal plane or heightened hole concentration in the Cu(2)O$_2$ planes resulted in a reduction of the lattice parameter, (c).

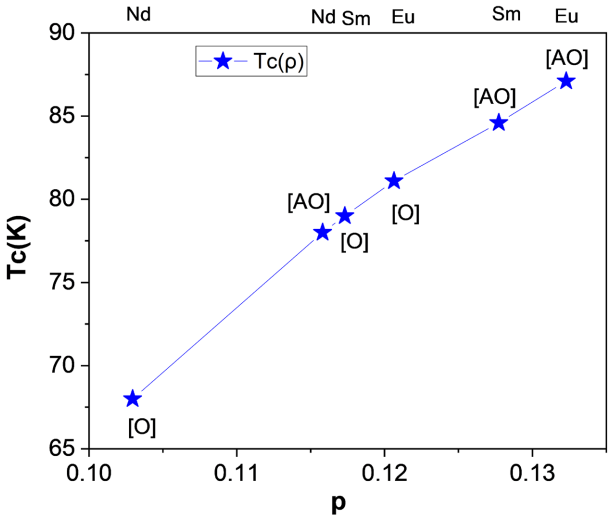

Figure 3. Tc as a function of the hole density (p) in the Cu(2)O$_2$ planes in LnSrBaCu$_3$O$_{6+z}$.

The superconducting critical temperature (Tc) and the lattice parameter (c) of the $LnSrBaCu_3O_{6+z}$ [AO] compound demonstrate an evident and inverse correlation with R (Ln^{3+}) as depicted in **Figure 5(a)** and **Figure 5(b)**, respectively. Run Zhao *et al.* [23] observed the variation of the critical temperature (Tc) and the lattice parameter (c) as a function of R (Ln^{3+}) in the $(YBa_2Cu_3O)_{1-x}$:$(BaZrO_3)_x$ compound, while systematically changing x from 0 to 0.4.

The Tc decreases with increasing c. This agrees with the expectation that large c value is accompanied by oxygen deficiency [24]. The justification for this is based on the increase in c correlated with a reduction in the number of p holes in the $Cu(2)O_2$ planes **Figure 4**.

Since the doping of these planes by holes, (p) is the result of increased oxygen content in the base plane. This is indicated by several searches [17] [18].

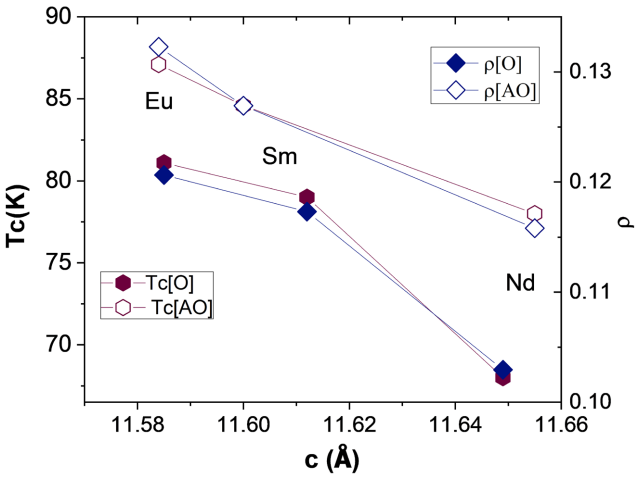

Figure 4. The correlation between the holes density (p) and the critical temperature (Tc) as a function of on the lattice parameter (c) and the heat treatment in $LnSrBaCu_3O_{6+z}$ (Ln = Eu, Nd, Sm).

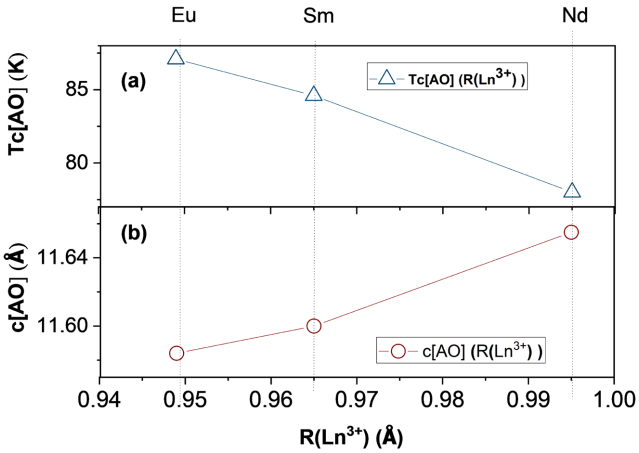

Figure 5. (a) Critical temperature (Tc) and (b) Lattice parameter (c) as a function of the ionic radius of the Ln rare earth in LnSrBaCu3O6+z [AO] (Ln = Eu, Nd, Sm).

Heat treatment [AO] (Figure 6) increases the surface (s [AO] > s [O]), volume (v [AO] > v [O]) and critical temperature (Tc [AO] > Tc [O]) of the $LnSrBaCu_3O_{6+z}$ compound for each Ln. The increase in volume can be attributed to the introduction of extra oxygen into the base plane, which leads to a rise in the number of oxygen atoms per chain. (displacement of the oxygen towards the axis b). The correlation depicted in this figure, relating the critical temperature (Tc) to the surface (s) and volume (v), indicates that the superconducting properties are present within the $Cu(2)O_2$ planes.

This correlation shows a relationship between the order of oxygen in the base plane and the doping, which corresponds to a transfer of the charges from the blocks of reserves toward the $Cu(2)O_2$ planes. Please note that the movement of the vacant site oxygen O(5) along axis (a) to the site O(4) along axis (b) occurs due to a greater lattice parameter b compared to lattice parameter a. This is due to the increase in oxygen number per chain, which also increases the critical temperature Tc [25]. Our maximum critical temperature (Tc [AO] = 71.1 K) is obtained in $EuSrBaCu_3O_{6+z}$ [AO] which correspond or optimal lattice parameter (b = 3.8695Å) compared, with the maximum lattice parameter b = 3.8872Å of Tc_{max} = 91.8 K obtained in case $YBa_2Cu_3O_{6+z}$ [26] for z = 0.96, and (b = 3.89Å, Tc = 89 K) in the $GdSrBaCu_3O_{6+z}$ compound for z = 0.93 [13]. Note here that the ratios of the a/b lattice parameters are almost equal (a/b [AO] = 0.982 Å ≈ a/b [26] = 0.983 Å ≈ a/b [13] = 0.984 Å), which shows a similar orthorhombic structure.

The orthorhombicity (ε), defined by the ratio (a − b)/(a + b), exhibited a significant increase from 0.38×10^{-3} for the sample [O] to 5.72×10^{-3} for the sample [AO] in $SmSrBaCu_3O_{6+z}$. This suggests a transition in the structural phase

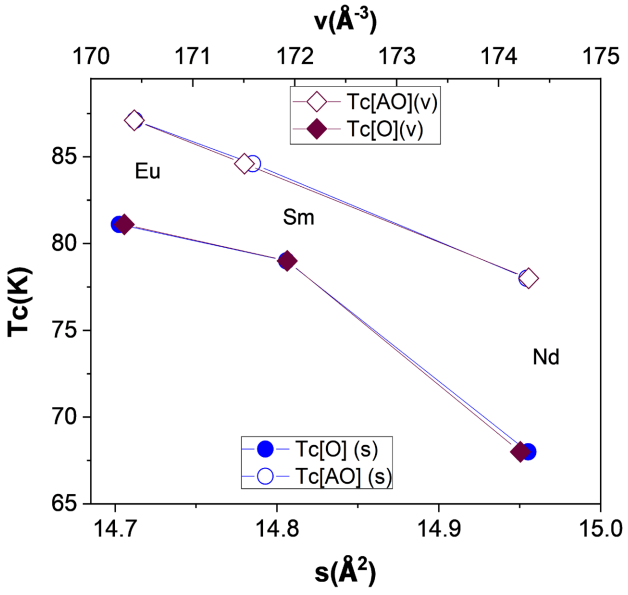

Figure 6. The critical temperature as a function of the volume, unit cell surface, and heat treatment. in $LnSrBaCu_3O_{6+z}$ (Ln = Eu, Nd, Sm).

from tetragonal to orthorhombic Figure 7. The variations in holes density (p) and orthorhombicity (ε) as a function of the critical temperature (Tc) are illustrated in the plot for $LnSrBaCu_3O_{6+z}$ [AO] (refer to Figure 7(b)). This makes it possible to say that the concentration of holes influenced by orthorhombicity. The rise in orthorhombicity indicates a notable increase in the number of oxygen atoms per chain (NOC). This increase can be attributed to the expansion of the b [AO] lattice parameter when compared to the a [AO] lattice parameter. Therefore, the critical temperature Tc has subsequently enhanced.

For each Ln element, the application of heat treatment [AO] leads to a notable increase in orthorhombicity (ε), hole density (p), and critical temperature (Tc) in $LnSrBaCu_3O_{6+z}$ (Ln = Eu, Nd, Sm).

When subjected to a specific heat treatment, the critical temperature of our sample is influenced by the ionic radius of the rare earth Ln. A noteworthy observation from Figure 8 is that the critical temperature exhibits a decrease trend as the ionic radius increases. This correlation highlights the significance of ionic radius in determining the critical temperature during the heat treatment process. Heat treatment [AO] increases Tc for each Ln.

The resistivity (ρ) of the samples, concerning their heat treatment [AO], is depicted in Figure 9(a) as a function of temperature.The data points for the large sample ionic radius are unmistakably situated below those of the small ionic radius. In all instances, ρ reaches zero at 76, 82, and 85 K, respectively, for the samples $NdSrBaCu_3O_{6+z}$ [AO], $SmSrBaCu_3O_{6+z}$ [AO], and $EuSrBaCu_3O_{6+z}$ [AO].

These values are in agreement with the results obtained from the AC susceptibility measurements. Please note that for a given set of samples, Tconset (χ') exhibits a superiority of 2 - 3 K over Tc ($\rho = 0$), while Tc (χ'') is approximately equal to Tc ($\rho = 0$). In its usual condition, the linear segment of ρ (T) follows the equation $\rho = \rho_0 + \alpha T$, where ρ_0 represents the residual resistance extrapolated to T = 0 K, and α represents the slope $d\rho/dT$. This relationship is obtained recently

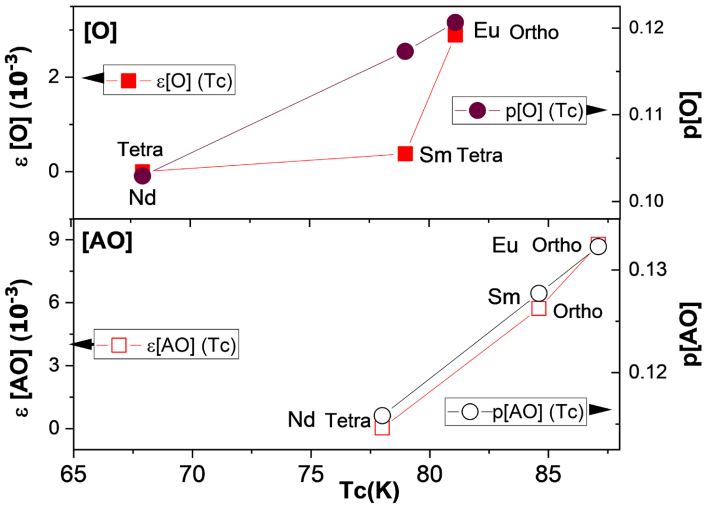

Figure 7. Orthorhombicity (ε) and holes density (p) as a function of critical temperature (Tc) for various heat treatments in $LnSrBaCu_3O_{6+z}$.

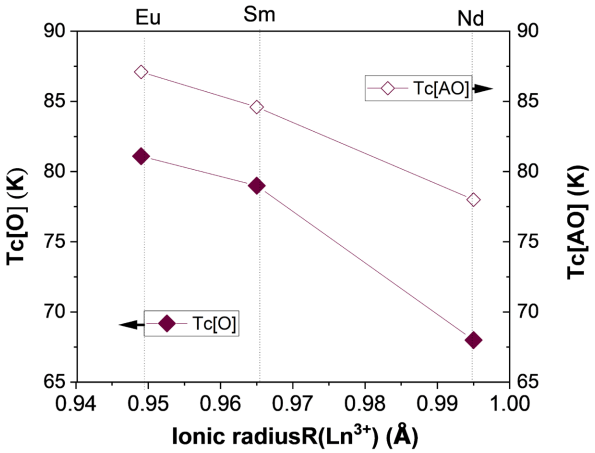

Figure 8. The critical temperature Tc as a function of ionic radius R (Ln^{3+}) and thermal processing in $LnSrBaCu_3O_{6+z}$.

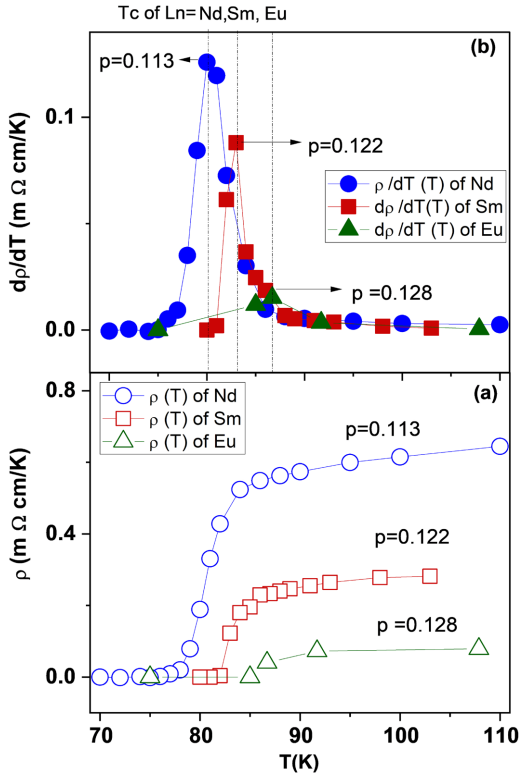

Figure 9. Plotting the resistivity (a) and derivative of the resistivity (b) as functions of temperature for of the samples $LnSrBaCu_3O_{6+z}$ [AO] (Ln = Eu, Nd, Sm).

by several authors in the case studies of the different types of superconducting oxides [27] [28] [29]. The slope α exhibits a noticeable decrease as we consider the ionic radius of the rare earth Ln, as illustrated in **Figure 9(a)**. This indicates a decrease of the normal electron interactions-phonons.

The rise in hole concentration within the $Cu(2)O_2$ planes led to noticeable changes in several key parameters as shown in **Table 2**. Specifically, it resulted in

Table 2. Superconducting and electrical parameters of $LnSrBaCu_3O_{6+z}$ [AO] (Ln = Eu, Nd, Sm). compounds.

Ln [AO]	Tc ($\rho = 0$) (K)	$\rho 0$ (μΩcm)	$\rho 295K$ (μΩcm)	α (μΩcm/K)
Nd	76	495	745	1.4
Sm	82	191	455	0.9
Eu	85	32	161	0.4

a decrease in α, ρ at 295 K, and ρ at 0 K, while simultaneously increasing Tc at p = 0. These observations highlight the significant impact of hole concentration on the material's electrical properties. The effect of the holes on these electrical and superconducting parameters is quite remarkable in several samples concerning the studies of these properties [30] [31].

The linear relationship between resistivity and temperature is a widely observed characteristic in cuprates [30] [31] [32]. These electric coefficients are specific to the $Cu(2)O_2$ planes and are influenced by hole doping, as shown in **Figure 9(a)**. This behavior is prevalent across various cuprate materials.

At elevated temperatures, the slope exhibits a reduction in correlation with the ionic radius. This phenomenon becomes more evident when observing the resistivity derivative with respect to temperature, as graphically depicted in the upper panel of **Figure 9**.

The reduction in p-hole doping leads to a notable enhancement in the peaks of the resistivity derivative concerning temperature ($d\rho/dT$). These changes are clearly depicted in **Figure 9(b)**, where the critical temperature of these peaks (Tp) is prominently observed. We have made a noteworthy observation in our systems where a single peak temperature (Tp) is evident, closely approaching the transition temperature. Of particular interest is the comparison between two specific systems: Eu [AO] and Nd [AO]. At a hole concentration of p = 0.128, corresponding to Eu [AO], we have observed a higher TP value of 86.7 K. In contrast, the Nd [AO] system, with a hole concentration of p = 0.113, exhibits a slightly lower TP value of 80 K. This disparity between the two systems adds an intriguing dimension to our findings. The data presented reveals a clear trend where curves shift towards lower temperatures as the ionic radius increases.

This observation strongly suggests that the introduction of Ln (lanthanide) elements into the Y sites of the $YSrBaCu_3O_{6+z}$ system has a significant impact on its superconducting properties. The aforementioned phenomenon was similarly noted in other doped systems where x > 0.01 in $Y_{1-x}Ce_xBa_2Cu_3O_{7-\delta}$ [33]. This observation is attributed to the higher ionic radius of cerium (Ce) compared to yttrium (Y). This decrease in (Tp) is also observed recently when (PbS) is added in $Bi_{1.6}Pb_{0.4}Sr_2CaCu_2O(PbS)_x$ [34]. Tp (x = 0) = 74 K decreases to Tp (x = 10) = 61 K, so adding the (PbS) increases the volume of this sample. Here, we compare the introduction of (PbS) with the increased ionic radius of the rare earth of our samples, which decreased Tp when it increased. Note here that the temperature

of peak Tp follows that of Tc.

4. Conclusions

The introduction of rare earth elements (Ln) in place of yttrium (Y) within the $YBaSrCu_3O_{6+z}$ systems has led to significant modifications in their structural, electrical, and superconducting properties. In heat treatment [O], different lanthanides (Ln) yield distinct structures: Nd results in a tetragonal structure, Sm leads to a pseudo-tetragonal structure, and Eu forms an orthorhombic structure. Additionally, these structures are accompanied by critical temperatures (Tc) of 68 K, 79 K, and 81.1 K, respectively. Heat treatment [AO] induces an enhancement in orthorhombicity while simultaneously leading to a reduction in the electrical parameters α, ρ_{295K}, and ρ_0. Further, it increased the Tc from 5.6 to 10 K depending on Ln. Each Ln element's ionic radius plays a significant role in influencing various properties. This specific approach led to a noteworthy outcome where the hole density in the $Cu(2)O_2$ planes increased. The observed correlation between hole concentration in these planes and the critical temperature adds further importance to these findings.

In our investigation, we have reached the conclusion that the critical temperature (Tc) is significantly influenced by various factors associated with the number of holes in the copper $Cu(2)O_2$ planes. Among these factors, the ionic size of the rare earth element Ln in $YBaSrCu_3O_{6+z}$, as well as its disorder on the site (Sr/Ba), have been found to play a crucial role. Additionally, factors such as the oxygen order in the chains, surface characteristics, atomic distances, heat treatment, and orthorhombicity also have a substantial impact on Tc.

It is worth noting that in our samples, the superconducting behavior is primarily governed by the density of holes present in the $Cu(2)O_2$ planes. This parameter emerges as a key determinant of the superconducting properties and represents an essential aspect in understanding the overall superconductivity in the system.

Conflicts of Interest

The authors declare no conflicts of interest regarding the publication of this paper.

References

[1] Bednorz, J.G. and Müller, K.A. (1986) Possible High T_c Superconductivity in the Ba-La-Cu-O System. *Zeitschrift für Physik B Condensed Matter*, **64**, 189-193. https://doi.org/10.1007/BF01303701

[2] Wu, M.K., Ashburn, J.R., Torng, C.J., Hor, P.H., Meng, R.L., Gao, L., Huang, Z.J., Wang, Y.Q. and Chu, C.W. (1987) Superconductivity at 93 K in a New Mixed-Phase Y-Ba-Cu-0 Compound System at Ambient Pressure. *Physical Review Letters*, **58**, 908-910. https://doi.org/10.1103/PhysRevLett.58.908

[3] Zhang, H. and Sato, H. (1993) Universal Relationship between T_c and the Hole Content in *p*-Type Cuprate Superconductors. *Physical Review Letters*, **70**, 1697-

1699. https://doi.org/10.1103/PhysRevLett.70.1697

[4] Liang, R., Bonn, D.A. and Hardy, W.N. (2006) Evaluation of CuO_2 Plane Hole Doping in $YBa_2Cu_3O_{6+x}$ Single Crystals. *Physical Review B*, **73**, Article ID: 180505.

[5] Reichardt, S., *et al*. (2018) Bulk Charge Ordering in the CuO_2 Plane of the Cuprate Superconductor $YBa_2Cu_3O_{6.9}$ by High-Pressure NMR. *Condensed Matter*, **3**, Article No. 23. https://doi.org/10.3390/condmat3030023

[6] Hücker, M., *et al*. (2014) Competing Charge, Spin, and Superconducting Orders in Underdoped $YBa_2Cu_3O_y$. *Physical Review B*, **90**, Article ID: 054514.

[7] Wang, X.Z., *et al*. (1992) Crystal Structure and Superconductivity in $REBaSrCu_3O_x$. *Physica C*: *Superconductivity*, **200**, 12-16. https://doi.org/10.1016/0921-4534(92)90316-5

[8] Sedky, A. and Youssif, M.I. (2016) Structural and Fluctuation Induced Excess Conductivity in R:1113 Superconductors. *Brazilian Journal of Physics*, **46**, 198-205. https://doi.org/10.1007/s13538-016-0401-z

[9] Awana, V.P.S., *et al*. (2000) Strong Dependence of Superconducting Transition Temperature (T_c) on the Rare Earth Ionic Size in $REBaSrCu_3O_7$ (RE = Y, Dy, Nd and La) Series. *Modern Physics Letters B*, **14**, 361-372. https://doi.org/10.1142/S0217984900000471

[10] Bellioua, M., Nafidi, A., Elkaaouachi, A., Nafidi, A. and Suryanarayanan, R. (2002) Enhancement of Orthorhombicity, T_c, Shielding and Irreversibility Line in Argon Preheated $Sm(SrBa)Cu_3O_{6+z}$. *Physica C*: *Superconductivity*, **383**, 183-190. https://doi.org/10.1016/S0921-4534(02)01323-0

[11] Rietveld, H.M. (1969) A Profile Refinement Method for Nuclear and Magnetic Structures. *Journal of Applied Crystallography*, **2**, 65-71. https://doi.org/10.1107/S0021889869006558

[12] Van der Pauw, L.J. (1958) A Method of Measuring the Resistivity and Hall Coefficient on Lamellae of Arbitrary Shape. *Philips Technical Review*, **20**, 220-224.

[13] Hellebrand, B., Gunasekaran, R., Steger, P. and Bäuerle, D. (1997) Structural and Superconducting Properties of Oxygen-Deficient $GdBaSrCu_3O_x$ ($6.5 < x < 7.0$). *Applied Physics A*, **65**, 235-240. https://doi.org/10.1007/s003390050572

[14] Almessiere, M.A., *et al*. (2020) Dimensionality and Superconducting Parameters of $YBa_2Cu_3O_7$-d/$(WO_3$ NPs$)_x$ Composites Deduced from Excess Conductivity Analysis. *Materials Chemistry and Physics*, **243**, Article ID: 122665. https://doi.org/10.1016/j.matchemphys.2020.122665

[15] Slimania, Y., *et al*. (2019) Improvement of Flux Pinning Ability by Tungsten Oxide Nanoparticles Added in $YBa_2Cu_3O_y$ Superconductor. *Ceramics International*, **45**, 6828-6835. https://doi.org/10.1016/j.ceramint.2018.12.176

[16] Bellioua, M., *et al*. (2017) Effect of the Number of Holes Psh and Heat Treatments on the Critical Temperature T_c in High T_c Superconductors. *International Journal of Engineering Research & Technology*, **6**, 393-398.

[17] Sederholm, L., *et al*. (2021) Extremely Overdoped Superconducting Cuprates via High Pressure Oxygenation Methods. *Condensed Matter*, **6**, Article No. 50. https://doi.org/10.3390/condmat6040050

[18] Cyr-Choiniere, O., *et al*. (2015) Two Types of Nematicity in the Phase Diagram of the Cuprate Superconductor $YBa_2Cu_3O_y$. *Physical Review B*, **92**, Article ID: 224502. https://doi.org/10.1103/PhysRevB.92.224502

[19] Sato, Y., *et al*. (2017) Thermodynamic Evidence for a Nematic Phase Transition at the Onset of the Pseudogap in $YBa_2Cu_3O_y$. *Nature Physics*, **13**, 1074-1078.

https://doi.org/10.1038/nphys4205

[20] Kistenmacher, T.J. (1988) Mapping the Orthorhombic-to-Tetragonal Transition at Ambient Temperature in $YBa_2Cu_3O_y$ Ceramics. *Journal of Applied Physics*, **64**, 5067-5070. https://doi.org/10.1063/1.342462

[21] Benzi, P., Bottizzo, E. and Rizzi, N. (2004) Oxygen Determination from Cell Dimensions in YBCO Superconductors. *Journal of Crystal Growth*, **269**, 625-629. https://doi.org/10.1016/j.jcrysgro.2004.05.082

[22] Dzul-Kifli, N.A.C., *et al*. (2022) Superconducting Properties of $YBa_2Cu_3O_{7-\delta}$ with a Multiferroic Addition Synthesized by a Capping Agent-Aided Thermal Treatment Method. *Nanomaterials*, **12**, Article No. 3958. https://doi.org/10.3390/nano12223958

[23] Zhao, R., Li, W., *et al*. (2014) Precise Tuning of $(YBa_2Cu_3O_{7-\delta})_{1-x}$:$(BaZrO_3)_x$ Thin Film Nanocomposite Structures. *Advanced Functional Materials*, **24**, 5240-5245. https://doi.org/10.1002/adfm.201304302

[24] Heinmaa, I., Lütgemeier, H., Pekker, S., Krabbes, G. and Buchgeister, M. (1992) Copper NMR and NQR in $YBa_2Cu_3O_x$ and $GdBa_2Cu_3O_x$ with x between 6 and 7. A Study of the Oxygen Ordering. *Applied Magnetic Resonance*, **3**, 689-709. https://doi.org/10.1007/BF03166290

[25] Milic, M., Matic, V.M. and Lazarov, N. (2011) The Dependence of Critical Temperature on Oxygen Concentration in $YBa_2Cu_3O_{6+x}$ in Terms of the Fragmented Chain Model. *European Journal of Physics*, **9**, 690-697. https://doi.org/10.2478/s11534-010-0060-6

[26] Casalta, H., *et al*. (1996) Neutron-Scattering Determination of the Structural Parameters versus Oxygen Content of $YBa_2Cu_30_{6+x}$ Single Crystals. *Physica C*: *Superconductivity*, **258**, 321-330. https://doi.org/10.1016/0921-4534(95)00674-5

[27] Sahoo, B., Routray, K.L., Panda, B., Samal, D. and Behera, D. (2019) Excess Conductivity and Magnetization of $CoFe_2O_4$ Combined with $Y_1Ba_2Cu_3O_{7-\delta}$ as a Superconductor. *Journal of Physics and Chemistry of Solids*, **132**, 187-196. https://doi.org/10.1016/j.jpcs.2019.04.035

[28] Loudhaief, N., Salem, M.B., Labiadh, H. and Zouaoui, M. (2020) Electrical Properties and Fluctuation Induced Conductivity Studies of Bi-Based Superconductors Added by CuS Nanoparticles Synthesized Through the Aqueous Route. *Materials Chemistry and Physics*, **242**, Article ID: 122464. https://doi.org/10.1016/j.matchemphys.2019.122464

[29] Hannachi, E., *et al*. (2021) Preparation and Characterization of High-T_c $(YBa_2Cu_3O_{7-\delta})_{1-x}$/$(CNTs)_x$ Superconductors with Highly Boosted Superconducting Performances. *Ceramics International*, **47**, 23539-23548. https://doi.org/10.1016/j.ceramint.2021.05.071

[30] Trabaldo, E., *et al*. (2022) Mapping the Phase Diagram of a $YBa_2Cu_3O_{7-\delta}$ Nanowire Through Electromigration. *Physical Review Applied*, **17**, Article ID: 024021. https://doi.org/10.1103/PhysRevApplied.17.024021

[31] Chen, Y.-J., *et al*. (2013) Superconducting Fluctuations and the Nernst Effect in High-T_c Superconductors. *Superconductor Science and Technology*, **26**, Article ID: 105029. https://doi.org/10.1088/0953-2048/26/10/105029

[32] Aliyev, V.M., Selim-Zade, R.I., Ragimov, J.A., Omelchenko, L.V. and Petrenko, E.V., *et al*. (2020) Analysis of Fluctuation Conductivity in $Y_{1-x}Cd_xBa_2Cu_3O_{7-\delta}$ ($x = 0$ - 0.4). *Low Temperature Physics*, **46**, 901-909. https://doi.org/10.1063/10.0001712

[33] Jurelo, A.R., Costa, R.M., Júnior, P.R. and Serbena, F.C. (2010) Fluctuation Conductivity and Phase Separation in Polycrystalline $Y_{1-x}Ce_xBa_2Cu_3O_{7-\delta}$ Superconduc-

tors. *Journal of Superconductivity and Novel Magnetism*, **23**, 247-252. https://doi.org/10.1007/s10948-009-0522-5

[34] Masnita, M.J., Awang, R. and Abd-Shukor, R. (2022) AC Susceptibility and Electrical Properties of PbS added $Bi_{1.6}Pb_{0.4}Sr_2CaCu_2O_8$ Superconductor. *Sains Malaysiana*, **51**, 315-328. https://doi.org/10.17576/jsm-2022-5101-26